Optical Engineering

SPIEDigitalLibrary.org/oe

Characterization of Talbot pattern illumination for scanning optical microscopy

Guangshuo Liu
Changhuei Yang
Jigang Wu

Characterization of Talbot pattern illumination for scanning optical microscopy

Guangshuo Liu
Shanghai Jiao Tong University
University of Michigan—Shanghai Jiao Tong University Joint Institute
Shanghai 200240, China

Changhuei Yang
California Institute of Technology
Department of Electrical Engineering
1200 East California Boulevard
Pasadena, California 91125

Jigang Wu
Shanghai Jiao Tong University
University of Michigan—Shanghai Jiao Tong University Joint Institute
Shanghai 200240, China
E-mail: jigang.wu@sjtu.edu.cn

Abstract. We studied the use of Talbot pattern illumination in scanning optical microscopy (SOM). Unlike conventional illumination spots used in SOM, the focal spots in Talbot pattern are more complicated and do not have a simple Gaussian intensity distribution. To find out the resolution of SOM using Talbot pattern, we characterized the evolution of the full-width-at-half-maximum spot size of the Talbot focal spots by computer simulation. We then simulated the SOM imaging under Talbot pattern illumination using the razor blade and the U.S. Air Force target as the sample objects, and compared the results with those performed with Gaussian spots as illumination. Using several foci searching algorithms, the optimal focal distances were found to be shorter than the theoretical Talbot distances. The simulation results were consistent with the experiment results published previously. We then provide a practical guidance for searching for optimal focal distances in the SOM based on these studies. [DOI: 10.1117/1.OE.52.9.091714]

Subject terms: Talbot effect; scanning optical microscopy; diffractive optics; autofocusing.

Paper 121759SS received Nov. 30, 2012; revised manuscript received Feb. 26, 2013; accepted for publication Mar. 4, 2013; published online Mar. 22, 2013.

1 Introduction

A two-dimensional (2-D) grid of focal spots is useful for implementing wide field-of-view (FOV) imaging with the principle of scanning optical microscopy (SOM).[1,2] Traditionally, the SOM is implemented using focal spots generated by microscope objectives[3] and these beams can be approximated as Gaussian beams. A large-area 2-D focal spots grid of Gaussian beams can potentially serve well in an SOM by providing parallel scanning capability. However, it is difficult to generate such a grid with good resolution (~1 μm or less) over areas beyond 1 mm. The Talbot effect provides a desirable approach to generate the focus grid.[1] It works by self-imaging an aperture grid without the help of lenses or other optical elements. As the aperture grid can be easily fabricated with microfabrication techniques, the device is mass producible and can be very low cost. Furthermore, the focal plane distance can be easily tuned by changing wavelength of the illumination beam,[1] and thus can provide microscopic images at different depth into a sample. Notice that the transmission efficiency will be very low if we use the aperture grid directly under illumination of a collimated beam since the aperture size is usually much smaller than the separation of adjacent apertures. Fortunately, the efficiency can be significantly improved by adding a microlens array before the aperture grid and focusing the beams at the apertures, or directly use the focus grid produced by the microlens array to generate Talbot spots if submicron resolution is not required.[4] Previously we have developed a scanning microscope implementation to achieve wide FOV imaging with resolution of ~1 μm using the Talbot pattern illumination.[1] In the experiment, it was observed that the optimal focal distance for imaging was a little shorter than the theoretically derived self-imaging distance. However, the Talbot focal spot is complicated and it's hard to determine the resolution and optimal focal plane of SOM using Talbot pattern illumination quantitatively. In this paper, we use diffraction based computer simulation to characterize the properties of Talbot focal spots and how it affects the imaging quality in SOM.

Talbot effect,[5] also known as self-imaging effect, reproduces the images of an arbitrary periodic mask at the integer multiples of a fixed distance. The Talbot distance Z_T can be calculated as

$$Z_T = 2d^2/\lambda, \tag{1}$$

where d is the spatial period of the mask and λ is the wavelength of illuminating beam. At the distance of

$$z = nZ_T/2, \qquad n = 1, 2, 3, \ldots \tag{2}$$

the Talbot images (when n is even) or phase-reversed Talbot images (when n is odd) of the mask will be generated. Using an aperture grid as the mask, we will be able to get the focus grid at the distance z. To avoid confusion with the term "Talbot distance" (Z_T), we will refer $nZ_T/2$ as "self-imaging distances" in the rest of the paper.

The derivation of Eqs. (1) and (2) are valid under paraxial approximation and when the aperture diameter is much larger than the wavelength.[6,7] In situations where those approximations are not valid, Talbot effect may still be observed. Yet, as was discovered in our previous experiment,[1] the best self-imaging positions would no longer be exactly located at distances described by Eq. (2).

In this paper, we present extensive computer simulation on the performance of Talbot-illumination-based microscopy and provide quantitative methods to precisely locate the

0091-3286/2013/$25.00 © 2013 SPIE

optimal focal distance for Talbot illumination. In Sec. 2, we briefly describe our simulation method and the evolving of Talbot pattern is demonstrated. In Secs. 3 and 4, we show the simulation of the SOM imaging of two samples: a razor blade structure and a U.S. Air Force (USAF) resolution target, with the same parameters as those in our previous experiments.[1] We were able to determine the optimal focal distance and theoretical resolution that can be achieved by looking at the simulated SOM images qualitatively. Finally in Sec. 5, we introduce a simple approach for searching the optimal focal distance quantitatively based on analysis of spot intensity distribution, and compare the results with two traditional autofocusing algorithms.

2 Evolving of Talbot Pattern

Our simulation employed the angular spectrum method,[8] which does not assume paraxial approximation. The simulation process is briefly explained as follows. For a monochromatic wave incident on the xy-plane and travels along z-direction, let $U(x,y,z)$ denote the optical wave disturbance. The angular spectrum of the wave at $z=0$ is then given by the Fourier transform of $U(x,y,0)$:

$$A\left(\frac{\alpha}{\lambda},\frac{\beta}{\lambda};0\right)=\int\int U(x,y,0)\exp\left[-j2\pi\left(\frac{\alpha}{\lambda}x+\frac{\beta}{\lambda}y\right)\right]\mathrm{d}x\mathrm{d}y, \tag{3}$$

where λ is the wavelength of incident wave, $\alpha=\lambda f_x$ and $\beta=\lambda f_y$ can be regarded as direction cosines of the corresponding plane wave component. Furthermore, the propagation of angular spectrum can be described as

$$A\left(\frac{\alpha}{\lambda},\frac{\beta}{\lambda};z\right)=A\left(\frac{\alpha}{\lambda},\frac{\beta}{\lambda};0\right)\exp\left(-j\frac{2\pi z}{\lambda}\sqrt{1-\alpha^2-\beta^2}\right)\times\mathrm{circ}(\sqrt{\alpha^2+\beta^2}), \tag{4}$$

where the function circ is defined as $\mathrm{circ}(r)=1$ (for $r\le 1$) and 0 (for $r>1$). By taking the inverse Fourier transform of $A(\alpha/\lambda,\beta/\lambda;z)$, we can then get the field distribution $U(x,y,z)$.

We used the above method to simulate the generated Talbot spots with an aperture grid as the mask. Here, we assume that the size of the aperture grid is infinite. In the simulation, the aperture grid had a spatial periodicity of 30 μm, and the transmission through each aperture was assumed to have a Gaussian distribution with the full width at half maximum (FWHM) of 0.8 μm. The wavelength of the illuminating beam was set as 700 nm. These parameters are consistent with the experiment described in Ref. 1. Figure 1 shows the evolving of the Talbot spots around $z=0.5Z_T$, $1.0Z_T$, and $1.5Z_T$ away from an aperture grid. The FWHM of the center spot of each diffraction pattern, calculated by Gaussian fitting, is listed below each spot pattern in Fig. 1 and plotted against the offset position (distance away from $z=0.5Z_T$, $1.0Z_T$, and $1.5Z_T$, respectively) in Fig. 2 explicitly.

According to Figs. 1 and 2, the evolving Talbot spot patterns have the following characteristics:

1. In general, the spot size increases as z approaches to the self-imaging distances, starting from $z=nZ_T/2-120$ μm. This increase is not a monotonic one, and it is possible for the spot to attain a small compact size if z is chosen carefully. On the other

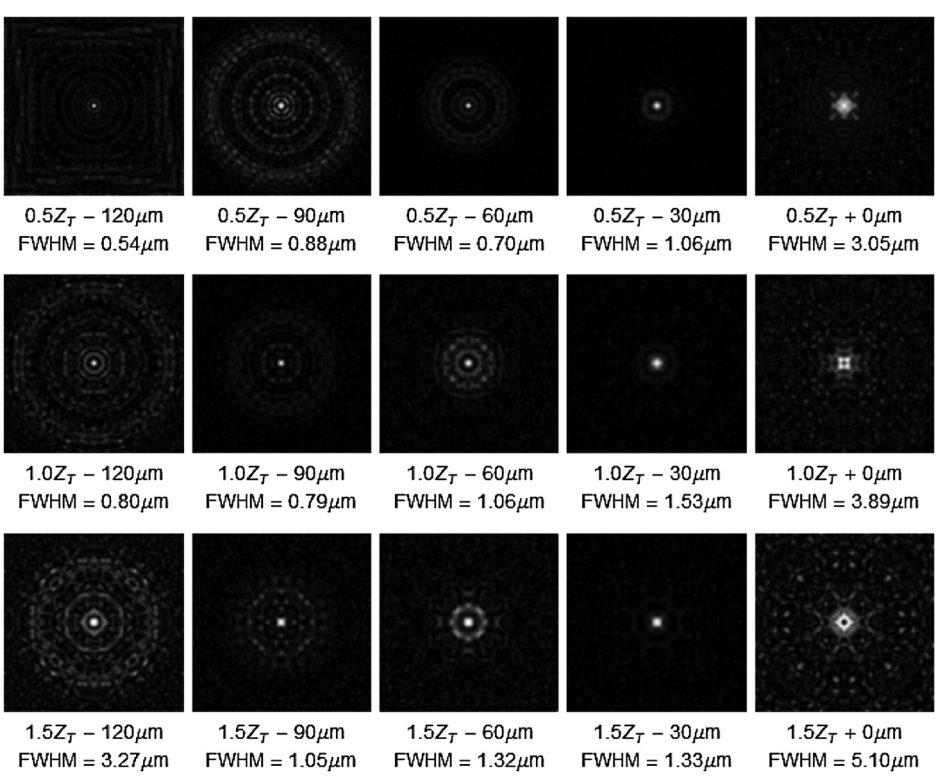

Fig. 1 Evolving of Talbot spot pattern around $0.5Z_T$, $1.0Z_T$, and $1.5Z_T$. The z-position and the FWHM are indicated under each spot pattern.

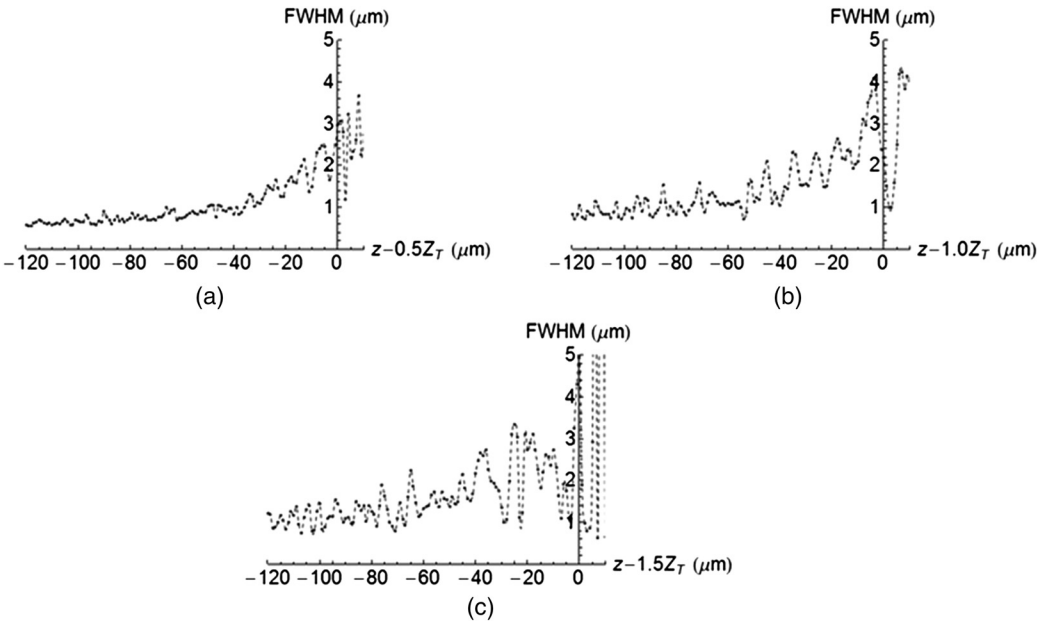

Fig. 2 FWHM spot size versus z offset position around (a) $0.5Z_T$, (b) $1.0Z_T$, and (c) $1.5Z_T$.

hand, being far in front of self-imaging distances does not always guarantee small spot, either. More briefly, the evolving is not exactly a monotonic variation in terms of spot size versus z. This is more obvious for the larger self-imaging distances.

2. In many cases, the spots are surrounded by intense rings.
3. As z moves positively beyond self-imaging distances, Talbot pattern become significantly distorted. The center spot might not even be observable.

In scanning microscopy, smaller spot provides potential capability to resolve finer details, while a reduced presence of surrounding rings can promote higher contrast. The two factors are both essential. Based on above observations, the imaging quality under Talbot spots illumination does not appear to evolve in a regular manner depending on either of the two perspectives. Thus, further study is necessary to find out the best focal distance.

3 Scanning of Razor Blade

To study the imaging quality under Talbot spots illumination, we first used an infinitely long binary razor blade as our sample, as shown in Fig. 3(a). The study will help us inspect the quality of the scanning microscopy on imaging boundaries in the sample, especially in situations where the dimension of sample details are much larger than the spot size.

In the simulation, we scanned the razor blade across a Talbot spot pattern, and calculated the transmission power by integrating the part of the spots, which is not blocked by the razor blade. Notice that we were simulating a Talbot spot grid for the scanning microscopy with a spatial periodicity of 30 μm; thus, the integration of the spots was calculated within a box of 30×30 μm. In each z-position, the scanning will give us a line signal. We can then get a 2-D image by putting the scan lines of different z-positions together, as shown in Fig. 3(b)–3(d), where the patterns around $0.5Z_T$, $1.0Z_T$, and $1.5Z_T$ are plotted versus the z-position. In the simulation, the scanning step was set as 0.06 μm, which was less than 1/10 of normal spot sizes.

By looking at the sharpness of the boundaries versus the z-position, we can see that the best quality of microscopy image occurs at tens of microns shorter than the self-imaging distances. We can also observe that there is a region of z-position that provides the sharpest edge, and the region is larger for larger self-imaging distances, with the trade-off of less sharpness in the boundary. This observation is further supported by the simulation in the following sections.

4 Scanning of U.S. Air Force Resolution Target

The USAF target is a well-accepted standard target for determining resolution of microscopic imaging. The target is normally composed of nine groups with line width ranging from 250 to ~0.8 μm. In the simulation, we used group 8 and 9 as our target, as shown in Fig. 4(a). The line widths of the target are listed in Fig. 4(b).

The simulation scheme of the SOM is shown in Fig. 4(c), where the USAF target is scanned under the illumination of the 2-D focus grid. The transmission of each focal spot is collected by a lens and imaged onto an imaging sensor. The transmission power of each focal spots is calculated by integration of the spot, partially blocked by the target, within a box of 30×30 μm according to the period of the focus grid. The line scans from each focal spots can then be combined to produce an image of the target. The simulation parameters were consistent with our previous experiment,[1] where the Talbot focal spots grid was tilted at an angle of 0.0167 rad with respect to the scanning direction of the USAF target. The sampling distance in both horizontal and vertical direction was 0.5 μm. In the simulation, the scanning z-position was ranging from $1.5Z_T - 120$ μm to $1.5Z_T$. Figure 5 shows the simulated scanning images. We can clearly see that the best focused image, with the best contrast, was obtained at $1.5Z_T - 30$ μm. In the following section, we quantitatively determine that $1.5Z_T - 29$ μm is in fact the optimal position. It agrees well with the simulation

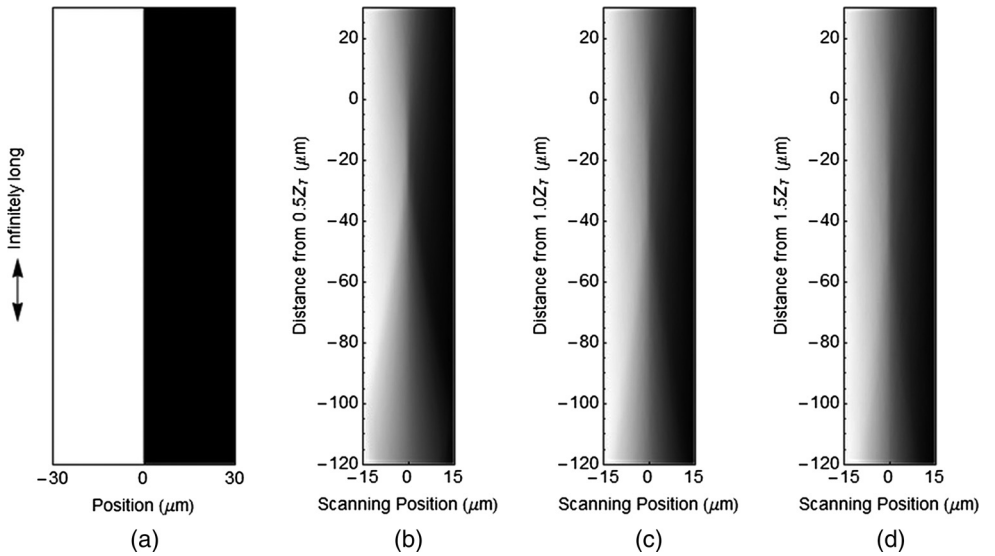

Fig. 3 Simulation of scanning of a single Talbot spot pattern across a razor blade. (a) the razor blade target; (b) the scanning pattern of razor blade around $0.5Z_T$; (c) the scanning pattern of around $1.0Z_T$; (d) the scanning pattern of the razor blade around $1.5Z_T$.

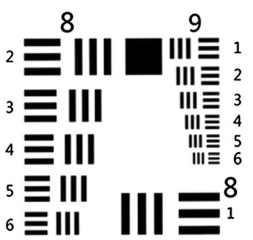

(a)

	Line width (μm)	
Element	Group 8	Group 9
1	1.95	0.977
2	1.74	0.870
3	1.55	0.775
4	1.38	0.690
5	1.23	0.615
6	1.10	0.548

(b)

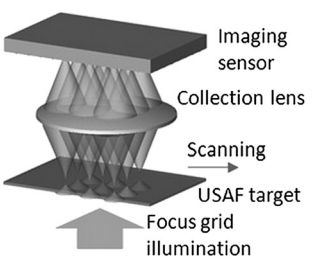

(c)

Fig. 4 (a) Group 8 and 9 of the U.S. Air Force (USAF) target; (b) line width of group 8 and 9 in the USAF target; (c) simulation scheme.

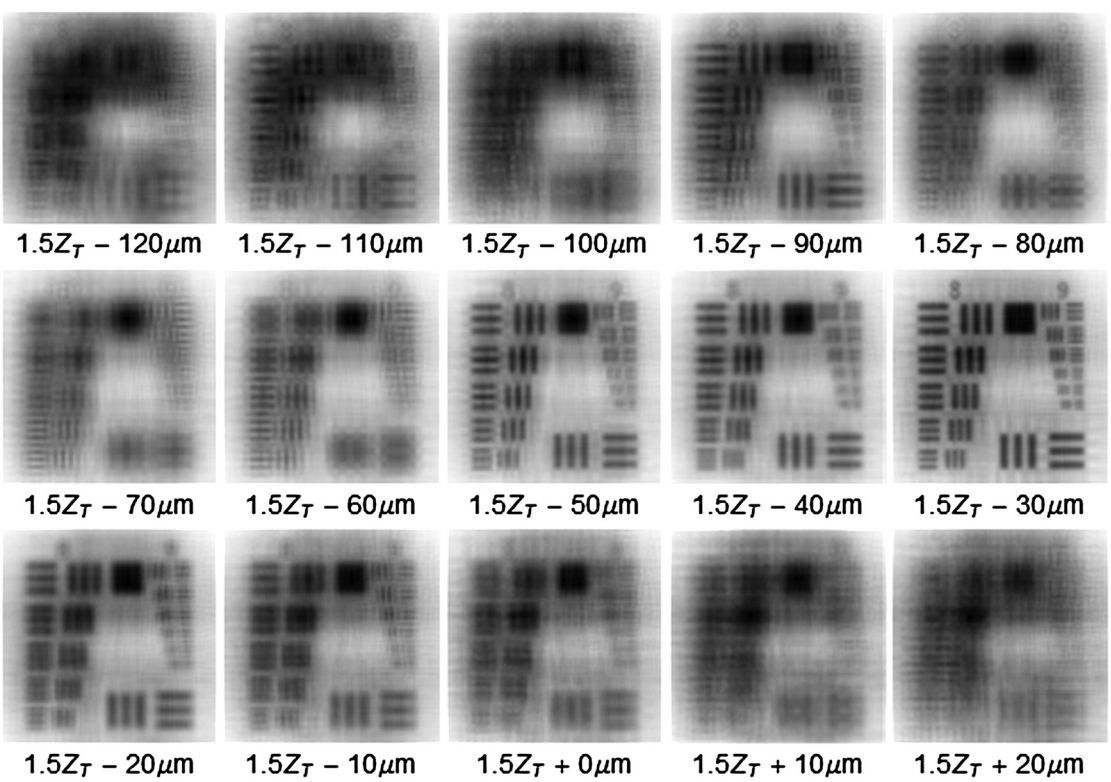

Fig. 5 Scanning images of the USAF target at z-positions ranging from $1.5Z_T - 120$ μm to $1.5Z_T$.

in Fig. 1, where the spot at $1.5Z_T - 30$ μm is relatively clean with very few surrounding rings and the size of spot is still rather small.

Interestingly, we also note that there are possibly multiple foci within a short spatial interval in Talbot pattern illumination. In this case, images around $1.5Z_T - 90$ μm has acceptable resolution, despite the relatively poor contrast compared with the best focused one at around $1.5Z_T - 30$ μm. This effect could be again explained by the spot patterns (Fig. 1) at $1.5Z_T - 90$ μm, which has a distinct and relatively small center spot, similar to the case at $1.5Z_T - 30$ μm. Yet, the rings are evidently more considerable, which accounts for the lower contrast. Also, because of the irregular variation of spot between $1.5Z_T - 90$ μm and $1.5Z_T - 30$ μm, we observe a short defocus region rather than a gradual improvement in image quality with respect to increasing z-position.

At $1.5Z_T - 29$ μm, we conducted a further simulation with smaller scanning step of 0.12 μm to examine the potentially highest resolution given by Talbot illumination, as shown in Fig. 6(a) and 6(b). We can see that the element 5 in group 9 can be well resolved and the last element is nearly resolved. Thus, we conclude that the SOM based on Talbot spot illumination with above parameters is capable to resolve details as good as ~0.6 μm.

For comparison, we simulated the scanning optical image of the USAF target by a focus grid of Gaussian beams at the waist, as shown in Fig. 6(c) and 6(d). The FWHM of the Gaussian was set as 0.8 μm according the original aperture size in the mask that producing the Talbot pattern. We can see that the scanning image of Gaussian beam have higher resolution and better contrast, which contribute to the smaller and cleaner Gaussian spot compared with the Talbot spot. Nonetheless, the Talbot spot still provides acceptable resolution and contrast.

5 Foci Searching Algorithms

In order to quantitatively determine the best z-position for scanning microscopy using Talbot illumination, we introduce three approaches to evaluate the image quality. They fall into two categories, namely statistical methods and autofocusing algorithms. The former ones are based on the simple idea that spots in the optimal focus grid are of minimum size and without surrounding rings. By direct analysis of intensity distribution, it is possible to achieve reasonable expectation on scanning quality. Approaches in the second category are self-explanatory—the images of best quality are benchmarked by edge sharpness. In such sense, even though the focusing process of Talbot-illumination-based microscopy is different from that in conventional optical microscopy, autofocusing algorithms should still be useful.

The first approach we propose belongs to statistical methods. It computes the focus measure F_{intfrac}, termed as intensity fraction, as the ratio of the intensity integral within a centered circle of certain radius R in the spot pattern to the intensity integral of the whole pattern. It intuitively indicates how well the intensity distribution is centralized in the Talbot pattern, which is directly related to scanning quality. With properly chosen R, it takes both contrast and resolution into consideration—a high F_{intfrac} implies both small spot size and insignificant existence of surrounding rings. We tried several R values, ranging from the original aperture radius (0.4 μm) to five times of that (2 μm). The simulation results show that three times (1.2 μm) is a proper choice and consistent with the observation of the scanning images qualitatively.

Figure 7(a) shows the focus curve, i.e., the intensity fraction F_{intfrac} versus the offset distance from $1.5Z_T$. We can see that approximately four peaks appear in the curve, occurring at around −115, −90, −49 and −30 μm away from $1.5Z_T$, respectively. These peaks match very well with the scanning results of both razor blade (Fig. 3) and USAF target (Fig. 5), in which the images of locally highest quality can be found at those positions. It is interesting and valuable to note that the infinitely long razor blade and USAF target with rather fine details are focused at very close positions. Such observation indicates that though the dimensions of details in samples may differ to a considerable extent, it should not affect our choice of optimal focal positions. This phenomenon is naturally true when using Gaussian spots for scanning, but not obvious for Talbot spots with complicated intensity distribution.

The next two approaches are both based on existing autofocusing algorithms, namely autocorrelation and Tenenbaum gradient. Autocorrelation has been proved to be the optimal algorithm for fluorescence microscopy by Santos et al.[9] And in a systematic comparison done by Sun et al.,[10] these two algorithms both have almost top performance among many other algorithms in terms of accuracy and noise immunity. There are comprehensive discussions on selecting optimal autofocusing algorithms for all types of microscopy other than the scanning microscopy. Here, we evaluate the two approaches for scanning microscopy with Talbot illumination by analyzing the simulation results.

Autocorrelation is based on the assumption that a detail is only visible if it contrasts with a neighboring detail.[11,12] It computes the focus measure as follows:

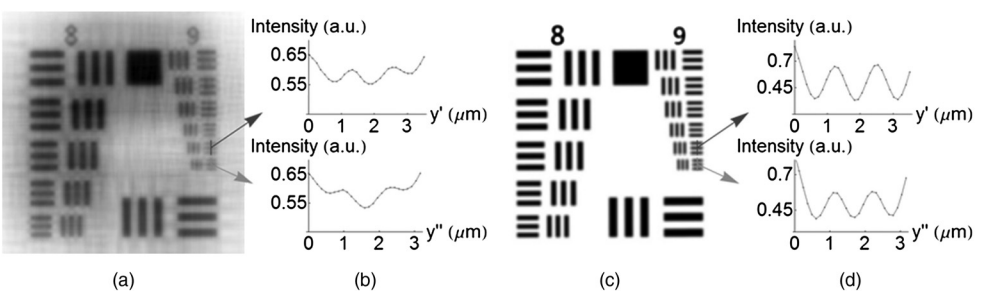

Fig. 6 (a) Scanning image of the USAF target at z-positions at $1.5Z_T - 29$ μm with a step-size of 0.12 μm; (b) the scan lines of element 5 and 6 of group 9 in (a); (c) scanning image of the USAF target by a Gaussian spot grid at the waist; (d) the scan lines of element 5 and 6 of group 9 in (c).

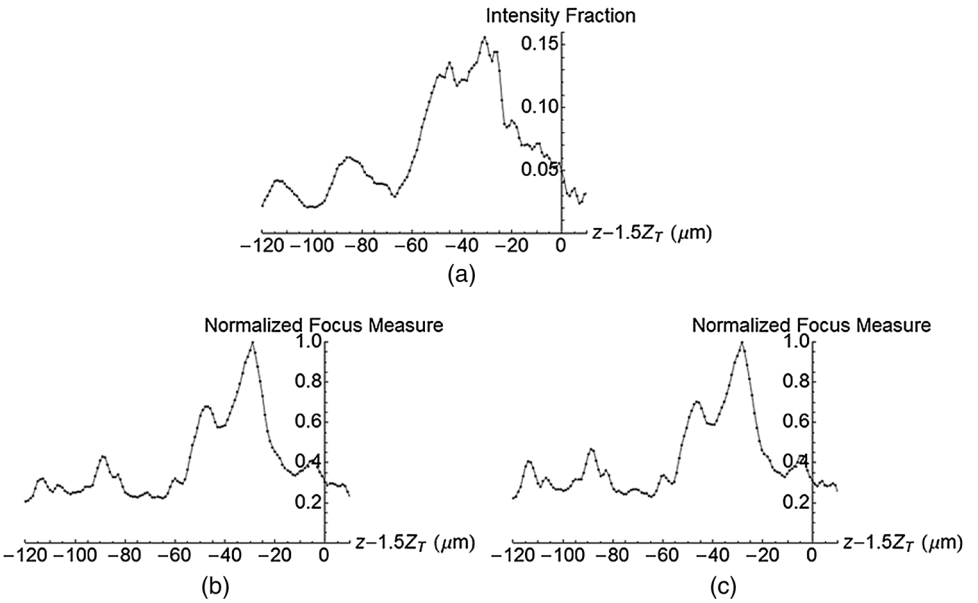

Fig. 7 Focus curve around $1.5Z_T$ by (a) intensity fraction method, (b) autocorrelation method, and (c) the Tenenbaum gradient method.

$$F_{\text{auto\_corr}} = \sum_{(i,j)} I(i,j)I(i+1,j) - \sum_{(i,j)} I(i,j)I(i+2,j), \tag{5}$$

Employing a similar idea as autocorrelation, yet implemented differently as derivative-based, Tenenbaum gradient[13,14] is given by

$$F_{\text{Tenen\_grad}} = \sum_{(i,j)} S_x(i,j)^2 + S_y(i,j)^2, \tag{6}$$

where S_x and S_y are the convolution of the image I with the Sobel operators as follows:

$$S_x = \begin{bmatrix} -1 & 0 & 1 \\ -2 & 0 & 2 \\ -1 & 0 & 1 \end{bmatrix} * I \quad \text{and} \quad S_y = \begin{bmatrix} -1 & -2 & -1 \\ 0 & 0 & 0 \\ 1 & 2 & 1 \end{bmatrix} * I. \tag{7}$$

The focus curves obtained by the autocorrelation and the Tenenbaum gradient methods are shown in Fig. 7(b) and 7(c), respectively. The two curves match each other very well. In addition, they also agree well with the intensity fraction method.

According to the results, we can see that autofocusing methods provide very reliable performance to locate foci positions accurately. Also the width of a peak is usually narrower and the global maximum is higher than those yielded via intensity fraction method. These are desirable advantages because it will be easier to determine the global optimal illumination position without getting trapped into local maxima. The disadvantage of autofocusing algorithms is that they are available only after the scanning is done for a range of z-positions, which usually takes a considerable amount of time. From this point of view, the intensity fraction method makes evaluation beforehand as long as one has the access to the intensity distribution profile of Talbot spot pattern, though may not provide result as good as the autofocusing algorithms. It is significantly more efficient. Based on the discussion above, in order to find foci positions quickly and accurately, it is preferable to make a compromise between the two types of approaches. In practice, we can first apply the intensity fraction method to obtain an acceptable spatial interval and then find the optimal focal position by performing scanning within this range and applying autofocusing algorithms.

6 Conclusions

We report extensive simulation on the performance of SOM using Talbot pattern illumination, with informative instructions for practical application. The resolution provided by Talbot-illumination-based scanning microscopy can be better than 1 μm and may possibly reach ~0.6 μm. The fact that the most effective Talbot spot pattern may not occur at self-imaging distances is further verified and studied. We find that dimension of details in the sample does not significantly affect the choice of focal distance. We also introduce several effective approaches to precisely determine the optimal focal distance, based on either directly analyzing the intensity distribution of spot pattern or traditional autofocusing algorithms. The studies in this paper are helpful for deeper understanding of SOM with non-Gaussian beams and also provide practical guidance for experimental alignment.

Acknowledgments

This work is supported by the National Science Foundation of China (Grant No. 61205192) and the Shanghai Pujiang Program (Grant No. 12PJ1405100).

References

1. J. Wu et al., "Focal plane tuning in wide-field-of-view microscope with Talbot pattern illumination," *Opt. Lett.* **36**(12), 2179–2181 (2011).
2. J. Wu et al., "Wide field-of-view microscope based on holographic focus grid illumination," *Opt. Lett.* **35**(13), 2188–2190 (2010).
3. R. Graf, J. Rietdorf, and T. Zimmermann, "Live cell spinning disk microscopy," *Adv. Biochem. Eng. Biotechnol.* **95**, 57–75 (2005).
4. S. Pang et al., "Wide and scalable field-of-view Talbot-grid-based fluorescence microscopy," *Opt. Lett.* **37**(23), 5018–5020 (2012).

5. H. F. Talbot, "LXXVI. Facts relating to optical science. No. IV," *Phil. Mag.* **9**(56), 401–407 (1836).
6. B. Besold and N. Lindlein, "Fractional Talbot effect for periodic microlens arrays," *Opt. Eng.* **36**(4), 1099–1105 (1997).
7. E. di Mambro et al., "Sharpness limitations in the projection of thin lines by use of the Talbot experiment," *J. Opt. Soc. Am. A* **21**(12), 2276–2282 (2004).
8. J. W. Goodman, *Introduction to Fourier Optics*, 3rd ed., Roberts & Company Publishers, Greenwood, Colorado (2004).
9. A. Santos et al., "Evaluation of autofocus functions in molecular cytogenetic analysis," *J. Microsc.* **188**(3), 264–272 (1997).
10. Y. Sun, S. Duthaler, and B. J. Nelson, "Autofocusing in computer microscopy: selecting the optimal focus algorithm," *Microsc. Res. Tech.* **65**(3), 139–149 (2004).
11. D. Vollath, "Automatic focusing by correlative methods," *J. Microsc.* **147**(3), 279–288 (1987).
12. D. Vollath, "The influence of the scene parameters and of noise on the behavior of automatic focusing algorithms," *J. Microsc.* **151**(2), 133–146 (1988).
13. E. Krotkov, "Focusing," *Int. J. Comput. Vis.* **1**(3), 223–237 (1987).
14. T. T. E. Yeo, S. H. Ong, and J. R. Sinniah, "Autofocusing for tissue microscopy," *Image Vis. Comput.* **11**(10), 629–639 (1993).

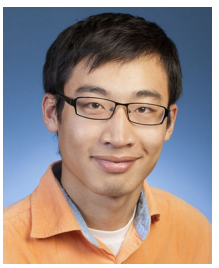

Guangshuo Liu received his BS degree in electrical and computer engineering from the University of Michigan—Shanghai Jiao Tong University Joint Institute, Shanghai, China, in 2012. He is now a PhD student in electrical and computer engineering at Carnegie Mellon University. His research interests include energy-aware computing and computer architecture. He is also interested in high-performance computing for biomedical imaging.

Changhuei Yang is a professor of electrical engineering and bioengineering at the California Institute of Technology. He conducts research in the area of chip-scale microscope, optofluidics, and time-reversal optical methods for deep tissue imaging. He has received the NSF Career Award, the Coulter Foundation Early Career Phase I and II Awards, and the NIH Director's New Innovator Award. Discover magazine included him as one of the top 20 scientists under 40 in its list of Best Brains in Science 2008.

Jigang Wu is an assistant professor at the University of Michigan—Shanghai Jiao Tong University Joint Institute, Shanghai, China. He received his BS and MS degrees in physics from Tsinghua University in 2001 and 2004, respectively, and PhD in electrical engineering from California Institute of Technology in 2008. His research interests include biomedical optical imaging and biophotonics with emphasis on developing novel imaging methods and seeking applications in biomedical research and clinical diagnosis.